



# Adsorption, initial growth and desorption kinetics of *p*-quaterphenyl on polycrystalline gold surfaces

S. Müllegger, O. Stranik, E. Zojer, A. Winkler\*

*Institute of Solid State Physics, Graz University of Technology, Petersgasse 16, A-8010 Graz, Austria*

Received 20 March 2003; received in revised form 1 July 2003; accepted 1 July 2003

## Abstract

Thermal desorption spectroscopy (TDS) and X-ray photoelectron spectroscopy (XPS) have been applied to investigate the kinetics of adsorption, layer growth and desorption of *p*-quaterphenyl (P4P) on polycrystalline gold surfaces. Two different desorption peaks resulting from a monolayer (wetting layer) and a multilayer can be observed. The multilayer predominantly grows in form of a continuous film at 93 K, whereas at room temperature needle-like island growth is observed. A rearrangement (island formation) of the continuous multilayer takes place during heating prior to desorption. The influence of carbon on the adsorption/desorption kinetics of the monolayer has been studied in detail. On the clean surface some amount of adsorbed P4P dissociates and hydrogen is released at about 650 and 820 K, respectively. No dissociation of P4P takes place on the carbon-covered surface. The intact P4P molecules of the monolayer desorb in form of two broad peaks around 420 and 600 K, the multilayer desorbs with zero order above 350 K. Quantitative measurements with a quartz microbalance yield a mean thickness of 0.27 nm for the monolayer, suggesting that the P4P molecules are lying flat on the surface, for both the clean and the carbon-covered surface.

© 2003 Elsevier B.V. All rights reserved.

**Keywords:** Thermal desorption spectroscopy; X-ray photoelectron spectroscopy; Adsorption kinetics; Sticking; Gold; Quaterphenyl; Thin film

## 1. Introduction

Thin organic films have attracted considerable interest in the recent past due to their promising features in optical, electro-optical and electronic devices. In particular, oligo-phenylenes have been studied extensively because they can be used to realize blue light emitting devices and thin film transistors [1–3]. Most frequently, thin organic films comprising “small” organic molecules (oligomeres) are produced by physical vapor deposition [4] or hot-wall epitaxy [5].

It is well known that the preparation parameters, like surface temperature, substrate conditions or deposition rate, determine the morphology and structure, and hence the electronic and optical properties of the grown layer [6–8]. In particular, the interface between the active organic material and the metal electrodes plays an important role [9]. There is some literature available concerning the structure of oligo-phenylenes (using X-ray diffraction [10–12] and low energy electron diffraction (LEED) [13]), the morphology (atomic force microscopy (AFM) and scanning tunneling microscopy (STM) [5,14,15], secondary electron microscopy [11] and fluorescence microscopy [13]) and the electronic structure [16–18]. However, there is still a lack of knowledge concerning the kinetics of

\* Corresponding author. Tel.: +43-316-873-8463;  
fax: +43-316-873-8466.  
E-mail address: [a.winkler@tugraz.at](mailto:a.winkler@tugraz.at) (A. Winkler).

layer formation of oligo-phenylenes on metal surfaces, in particular in the monolayer and beginning multilayer regime. For other large organic molecules comparable investigations on the kinetics of adsorption, ordered layer growth and desorption on surfaces are available (e.g. PTCDA [19,20], NTCDA [21], NDCA [22], ECnT [23], acenes [24], sexithienyl [25]).

In this work, we focus on the adsorption, initial growth and desorption of *p*-quaterphenyl (P4P) on/from clean and carbon-covered polycrystalline gold surfaces. Polycrystalline gold was chosen for these investigations because it has some relevance for application as contacting electrodes in organic based optoelectronic devices. We will demonstrate that significant dissociation of P4P in the monolayer regime occurs on such surfaces during sample heating, which influences further adsorption and the growth kinetics. Thermal desorption spectroscopy (TDS) and X-ray photoelectron spectroscopy (XPS) were the main techniques used for the kinetics experiments.

## 2. Experimental

The experiments were carried out in a UHV chamber with a base pressure of  $\approx 10^{-10}$  mbar. The apparatus was equipped with an Auger electron spectrometer (AES), an X-ray photoelectron spectrometer and an in-line quadrupole mass spectrometer (QMS). Evaporation of *p*-quaterphenyl was accomplished by a Knudsen cell made of quartz glass. The support for the Knudsen cell was water cooled, in particular during

baking of the UHV system, to avoid uncontrolled evaporation. A quartz microbalance was permanently positioned about  $30^\circ$  off-axis relative to the Knudsen source-sample direction. This allows the continuous control of the evaporation flux. For calibration of the impingement rate on the sample, the sample was temporarily replaced by a second quartz microbalance. For the calculation of the mean thickness of P4P evaporated on the surface we have used the bulk density  $\rho = 1.25 \text{ g/cm}^3$  [26].

Fig. 1 shows the unit cell of the crystalline form of P4P at room temperature [27,28]. In the gas phase, the collinear phenyl rings are tilted with respect to each other by an angle of  $30\text{--}40^\circ$  due to repulsion between the *ortho*-hydrogen atoms. In the crystalline phase the arrangement of the phenyl rings is nearly planar on average [18]. The crystal structure of P4P at 300 K is monoclinic and the crystal unit cell contains two molecules. The bulk lattice constants are  $a = 0.811 \text{ nm}$ ,  $b = 0.561 \text{ nm}$ ,  $c = 1.791 \text{ nm}$ , the monoclinic angle  $\beta = 95.80^\circ$ , and the symmetry is  $P2_1/a$  [26].

The sample, a high purity (99.99%) polycrystalline gold foil ( $10 \text{ mm} \times 10 \text{ mm} \times 0.1 \text{ mm}$ ), was spot-welded onto two Ta-wires, which were clamped into Cu-electrodes. This allowed ohmic heating of the sample up to 1000 K and cooling to 93 K, via a LN<sub>2</sub> cold finger. The temperature was measured with a NiCr–Ni thermocouple spot-welded to the Au-foil.

For the investigation of the adsorption and desorption kinetics mainly thermal desorption spectroscopy was applied. Typical heating rates of 1 K/s were used and the spectra were taken with an in-line quadrupole

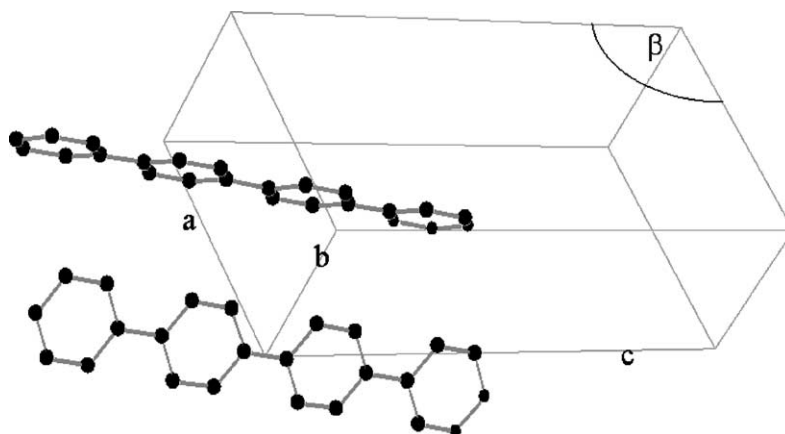


Fig. 1. Crystallographic structure of P4P in the condensed phase at room temperature.

mass spectrometer (0–512 amu). The molecular mass 306.4 amu of the intact P4P was mainly measured, but in some cases the mass 153 amu was taken as being representative of P4P, using a mass spectrometer 0–200 amu. This was done when the 512 amu mass spectrometer was not yet available. We have carefully checked that this signal is also representative of the P4P molecule by comparing the desorption spectra for different cracking products (153, 138 and 77 amu) with the spectra of the intact molecule. The shape of all spectra was the same, indicating that they were the cracking products of one desorbing species.

One important point in this context is the chemical composition of the polycrystalline gold surface as used for the experiments. Cleaning of the gold surface is in principle rather easy: Short sputtering with  $\text{Ar}^+$  ions (10 min,  $p = 5 \times 10^{-5}$  mbar) and annealing at 900 K is sufficient to obtain a clean Au surface, as verified by Auger electron spectroscopy. However, adsorption of quaterphenyl on a clean surface and subsequent desorption leads to some dissociation and consequently to a contamination with carbon. This carbon uptake is very fast but levels off at a carbon coverage of about  $6 \times 10^{14}$  C-atoms/cm<sup>2</sup> (as described below in more detail). This is probably due to dis-

sociation of P4P at defect sites on the polycrystalline surface and/or on high index surface planes of the individual crystallites. In fact, on the low indexed Au(1 1 1) surface no significant dissociation of P4P can be seen [29]. In addition to that, intentionally extensive irradiation (few hours) of a thick P4P film (10 nm) by X-rays also leads to dissociation of P4P. By this method a carbon saturation layer of about  $1.2 \times 10^{15}$  C-atoms/cm<sup>2</sup> (one monolayer) can be prepared. The increase of the X-ray induced carbon on the surface, however, is very slow compared with that caused by dissociation. During XPS experiments no significant X-ray induced C contamination could be observed.

### 3. Results and discussion

#### 3.1. TDS measurements

Thermal desorption spectroscopy has been applied to reveal the desorption kinetics of P4P from polycrystalline gold surfaces (heating rate  $\beta = 1$  K/s). It turned out that some amount of the adsorbed quaterphenyl dissociates during sample heating. In Fig. 2 we

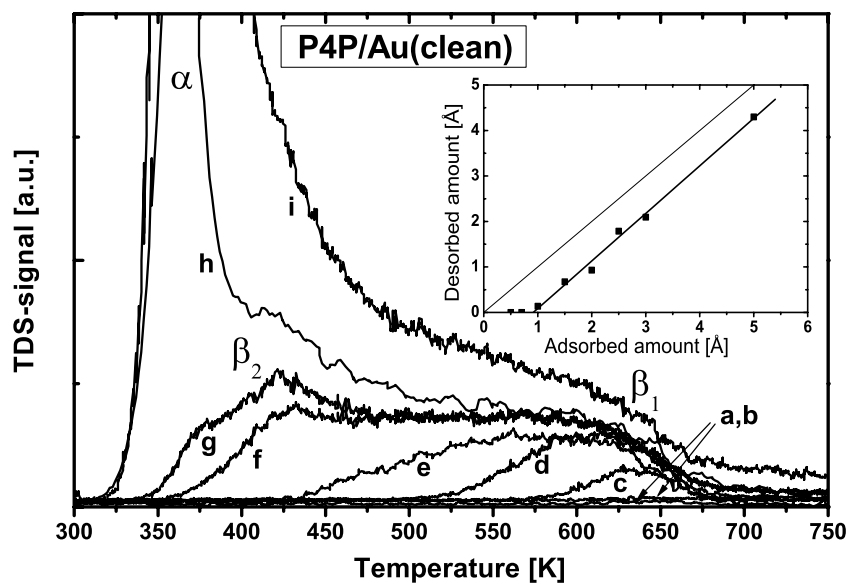


Fig. 2. Thermal desorption spectra for P4P from the clean polycrystalline gold surface. Adsorption temperature: 93 K. The parameter is the initially adsorbed amount of P4P, indicated in form of the mean thickness: (a) 0.05 nm, (b) 0.07 nm, (c) 0.1 nm, (d) 0.15 nm, (e) 0.2 nm, (f) 0.25 nm, (g) 0.3 nm, (h) 0.5 nm, (i) 2 nm. The insert shows the relation between desorbed and adsorbed amount of P4P, indicating the dissociation of a P4P quantity of about 0.1 nm.

present TD spectra for P4P where the surface was always cleaned by sputtering and annealing prior to exposure (adsorption temperature  $T_{\text{ads}} = 93$  K). One can see that after evaporation of up to 0.07 nm P4P on the surface (curves a and b) no desorption of intact P4P appears. Only after higher doses of P4P desorption of the intact molecules commences. From a plot of the desorbed amount of P4P as obtained from TDS versus the adsorbed amount as obtained by the quartz microbalance (see insert Fig. 2) one finds that a quantity of about 0.1 nm P4P is always missing in desorption. We can attribute a carbon coverage of  $6 \times 10^{14}$  atoms/cm<sup>2</sup> to this quantity of dissociated P4P. This corresponds to half a monolayer of carbon, if we assume a mean density of atoms on the polycrystalline gold surface of  $1.2 \times 10^{15}$  atoms/cm<sup>2</sup>.

The desorption peak which appears for small coverage at about 630 K (adsorption of 0.1 nm P4P) will be referred to as  $\beta_1$ -peak. With increasing coverage this peak shifts strongly to lower temperature. A second peak ( $\beta_2$ ) arises at a desorption temperature of about 430 K. Both broad and overlapping peaks saturate at about 0.27 nm mean thickness before a sharp peak arises in the temperature range of 330–400 K, which does not saturate. We associate the broad (double) peak up to a mean thickness of 0.27 nm with adsorption into the monolayer. The large temperature shift of each of the two monolayer peaks might be partially due to the manifold of different adsorption configurations possible on a polycrystalline surface, but it is most probably due to strong repulsive forces acting in the monolayer. This is corroborated by the fact that P4P on a Au(1 1 1) single crystal surface also exhibits two similar desorption peaks for the monolayer [29]. It is therefore tempting to correlate the two desorption peaks with two distinct adsorption sites of P4P in the monolayer.

Determination of the desorption energy from the desorption spectra is complicated in the case of overlapping and strongly shifting peaks. The evaluation of the whole set of spectra by the complete method of King [30] or by some other refined evaluation methods [31], which are all based on a single Polanyi–Wigner equation, is not meaningful. In such a case often a rough guess of the desorption energy  $E_d$  is made just from the peak maxima of single spectra ( $T_p$ ), according to the formula by Redhead [32] for first-order desorption ( $E_d = kT_p(\ln(vT_p/\beta - 3.64))$ ). This yields a

desorption energy of 1.8 and 1.2 eV for the high (630 K) and low (425 K) temperature peaks, respectively. A frequency factor ( $v$ ) of  $1 \times 10^{13}$  s<sup>-1</sup> has been assumed in this case. However, one should have in mind that frequency factors for desorption of large organic molecules can deviate from this value by orders of magnitude [33,34].

A sharp desorption peak ( $\alpha$ ) arises around 360 K after saturation of the monolayer and increases continuously with increasing P4P exposure. From this fact and from the peak shape (see also Fig. 5) we can attribute this peak to desorption from the multilayer (zero-order desorption). In this case, the desorption energy can be easily calculated from the slope of the plot  $\ln(\text{rate})$  versus  $1/T$  [31]. A desorption energy of 1.61 eV and a pre-exponential factor of  $3.7 \times 10^{35}$  cm<sup>-2</sup> s<sup>-1</sup> has been obtained for the multilayer. This is in good agreement with the literature value of 1.62 eV for the sublimation enthalpy of P4P [35].

In order to investigate the dissociation of P4P at low coverage in more detail we have searched for possible cracking products by multiplexed TDS. The only desorption product we have observed, in addition to P4P, was hydrogen. Fig. 3 shows the spectra for the masses 306 and 2 after adsorption of 0.2 nm P4P on the clean gold surface. Two distinct hydrogen desorption peaks are observed, at 650 and 820 K, respectively, which are already saturated in this case. Beginning with very low P4P coverage, first the high temperature peak (B) appears and increases proportional to the amount of adsorbed P4P between 0 and 0.07 nm mean thickness. In this coverage regime no P4P desorption is observed. The amount of carbon left behind on the surface, corresponding to the saturation of the B peak, is  $4 \times 10^{14}$  atoms/cm<sup>2</sup>. With an increasing amount of adsorbed P4P, intact P4P molecules start to desorb, but simultaneously a second, low temperature hydrogen peak (A) arises, just above the desorption temperature of P4P. The intensity of this peak increases proportional to the amount of P4P desorbing as  $\beta_1$ . A further increase of the P4P coverage into the full monolayer ( $\beta_1 + \beta_2$ ) and into the multilayer regime has no more influence on the hydrogen desorption features. From a comparison of the peak areas for the A and B peaks we obtain a total carbon coverage of  $6 \times 10^{14}$  atoms/cm<sup>2</sup>, left behind on the surface due to dissociation of P4P. The chemical nature of this carbon was checked by XPS.

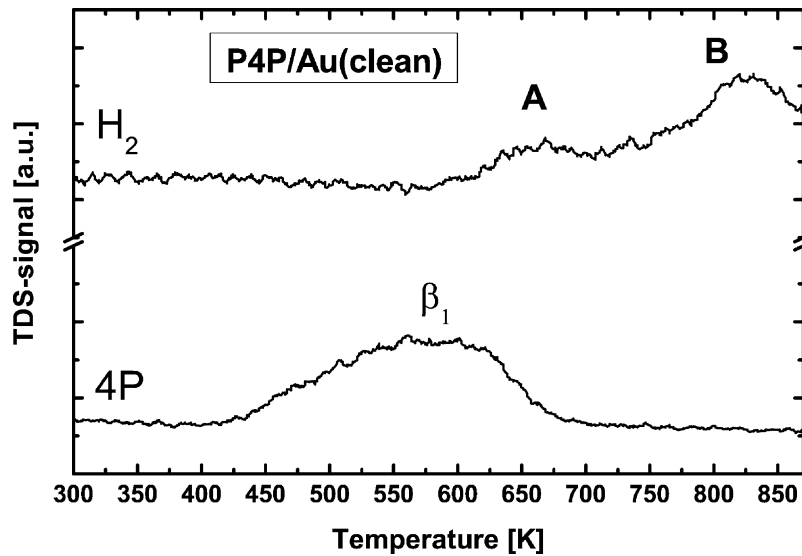


Fig. 3. Multiplexed TDS for hydrogen and P4P, after adsorption of 0.2 nm of P4P on the clean Au surface at room temperature.

A binding energy of the C 1s signal of 284.4 eV (see below) is an indication of a graphitic like carbon [36].

From the results described above and the observed TDS spectra for P4P and H<sub>2</sub> we can draw the following conclusions for the monolayer adsorption. P4P adsorbs on a clean polycrystalline gold surface at least in form of three different states. For a coverage of up to 0.07 nm P4P is so strongly bound to the surface that no desorption of the intact molecule takes place. It rather dissociates at about 820 K completely and pure hydrogen is released (peak B). P4P molecules adsorbed in a coverage range between 0.07 and 0.15 nm desorb in the temperature range of 500–650 K ( $\beta_1$ ). However, a fraction of the molecules in this adsorption state again dissociates completely and hydrogen is released in the temperature range of 600–700 K (peak A). The residual carbon of about 1/2 monolayer is of graphitic type. P4P molecules adsorbed between 0.15 and 0.27 nm mean thickness desorb intact in a temperature range of 350–500 K as  $\beta_2$  monolayer peak. For higher coverage, desorption from the multilayer takes place.

Due to the dissociation of P4P in the sub-monolayer region at elevated temperature, for practical purposes one will probably often deal with carbon contaminated polycrystalline gold surfaces. We have therefore also studied the adsorption/desorption kinetics of P4P on the carbon-covered gold surface. Fig. 4 shows desorption spectra for P4P from a gold surface, which

was always covered with a stable carbon layer of  $6 \times 10^{14}$  atoms/cm<sup>2</sup> prior to adsorption. In Fig. 4, one can again distinguish between two different desorption features in the monolayer regime. However, the high temperature peak for the monolayer ( $\beta_1$ ) is now strongly suppressed and there is only one pronounced, but still rather broad peak in the 400 K range. In addition to that, no dissociation of P4P takes place on the carbon-covered surface (no hydrogen release). There is now a strict proportionality between the desorbed amount as obtained from integration of the TD spectra and the adsorbed amount as obtained from the quartz microbalance (see also Fig. 6). However, for the clean and the carbon-covered gold surface the monolayer (the wetting layer) saturates at the same mean nominal thickness of about 0.27–0.3 nm. This is about half of the *b*-axis of the monoclinic P4P crystal, which is an indication that the P4P molecules are lying rather flat on the surface in the monolayer regime.

For the carbon-covered gold surface we have investigated the multilayer desorption up to a mean thickness of 12 nm (Fig. 5). The desorption peaks appearing in this case exhibit clearly zero-order desorption characteristics: A common leading edge, peak maxima shifting to higher temperature with increasing coverage, and a sharp cut-off at high temperature. The calculation of the desorption energy as described above yields a value of 1.64 eV. Apparently, the

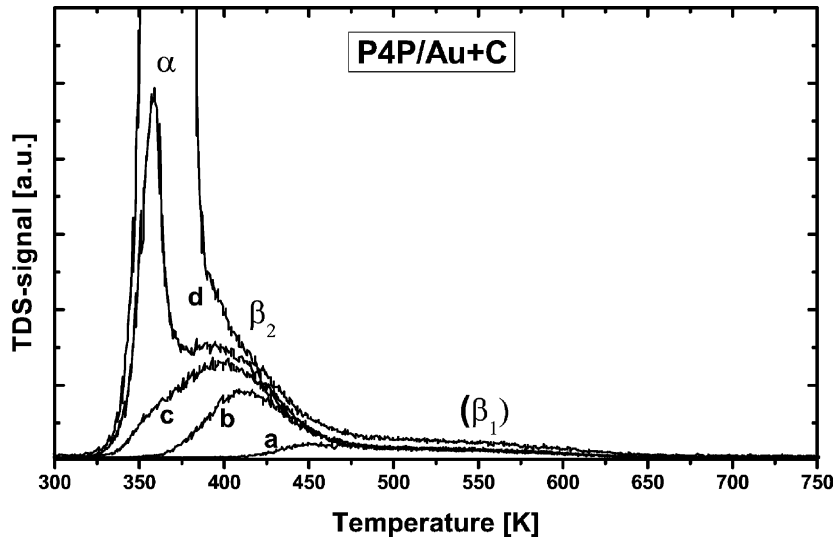


Fig. 4. Thermal desorption spectra for P4P from the polycrystalline gold surface, covered with  $6 \times 10^{14}$  C-atoms/cm<sup>2</sup>. Adsorption temperature: 300 K. The parameter is the initially adsorbed amount of P4P, given by the mean thickness. (a) 0.1 nm, (b) 0.2 nm, (c) 0.3 nm, (d) 0.4 nm, (e) 2 nm.

desorption from the multilayer is not significantly influenced by the initial condition of the gold surface (clean or carbon covered). There is, however, the puzzling result that the desorption energy for the  $\beta_2$  monolayer state calculated according to Redhead [32]

is smaller than that for the multilayer, although it appears at higher temperature in TDS. This shows the weakness of the method after Redhead, where a particular frequency factor has to be assumed for evaluation of the desorption energy.

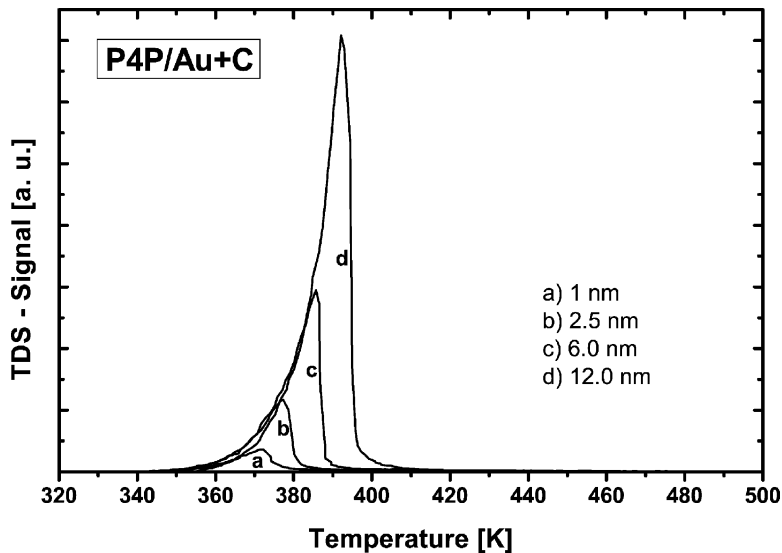


Fig. 5. Thermal desorption spectra for high coverage of P4P from the polycrystalline gold surface (multilayer desorption). Adsorption temperature: 300 K. The parameter is the initially adsorbed amount of P4P, given by the mean thickness.

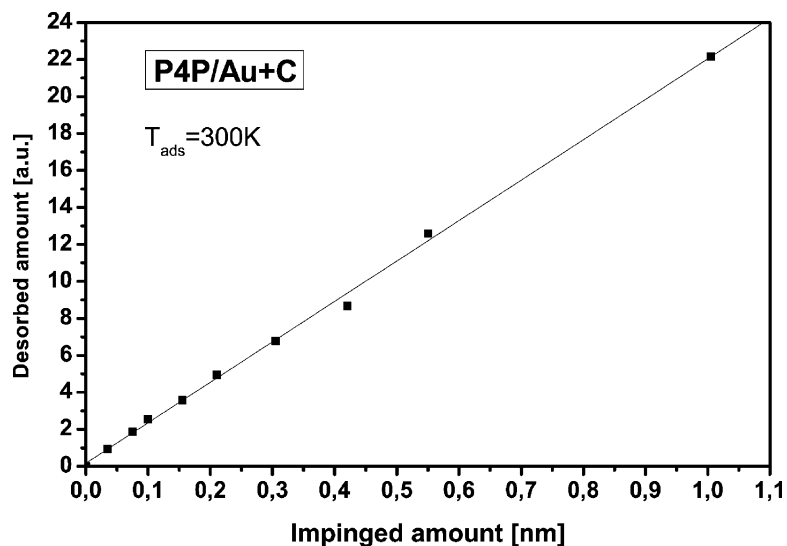


Fig. 6. Integrated desorption spectra versus the amount of impinged P4P molecules on the carbon-covered gold surface, as determined in situ by a quartz microbalance.

From thermal desorption data, we have also determined the sticking coefficient for P4P adsorption at room temperature and at 93 K, as a function of coverage in the mono- and multilayer regime. In Fig. 6, the adsorbed amount, as measured by thermal desorption spectroscopy, is plotted versus the impinged amount, as measured during evaporation by the calibrated quartz microbalance held at room temperature. A similar result is obtained for a sample temperature of 93 K. These experiments have been performed on the carbon pre-covered gold surface where no dissociation of P4P takes place. For both adsorption temperatures, we observe a close to linear relationship between offered and adsorbed amount of P4P over a broad coverage range. The observation that the sticking coefficient is independent of coverage and temperature suggests that the sticking coefficient is unity in all cases.

### 3.2. XPS experiments

The next issue concerns the adsorption and layer formation of P4P during adsorption. Layer-by-layer, island or Stranski–Krastanov (SK) growth are the most frequently observed growth modes. In TDS, we observe a clearly separated monolayer and multilayer desorption peak. But no statements can be made as to the multilayer formation during adsorption. To shed

light on this issue we have measured the change of the C 1s signal and the Au 4f<sub>7/2</sub> signal in XPS during P4P adsorption on the carbon-covered gold surface, as shown in Fig. 7. The binding energy of the C 1s signal for this carbon species is 284.4 eV. This corresponds to the binding energy of carbon in graphitic form. The binding energy of the C 1s signal does not change significantly upon adsorption of P4P on the surface, even in the very low P4P coverage range where a transition from the monolayer to the multilayer takes place. The 284.4 eV are in accordance with the C 1s signal in a number of XPS studies on aromatic and conjugated hydrocarbons [9,37,38].

Fig. 8 shows the change of the C 1s and Au 4f XPS signal intensities as a function of the mean thickness of the P4P layer, as measured by the calibrated quartz microbalance, for a sample temperature of 93 K. One observes an increase of the C 1s signal and an exponential decrease of the underlying substrate signal Au 4f. This is a clear evidence for a continuous layer-like growth of P4P at this temperature. From the slope of the straight line in the plot  $\ln(\text{Au } 4f\text{-signal})$  versus thickness we calculate a mean free path of the Au 4f<sub>7/2</sub> electrons ( $E_{\text{kin}} = 1170$  eV) in P4P of  $\lambda = 2.4 \pm 0.3$  nm. The important observation in Fig. 8 is, that already at a mean thickness of about 17 nm the signal of the underlying substrate is completely suppressed.

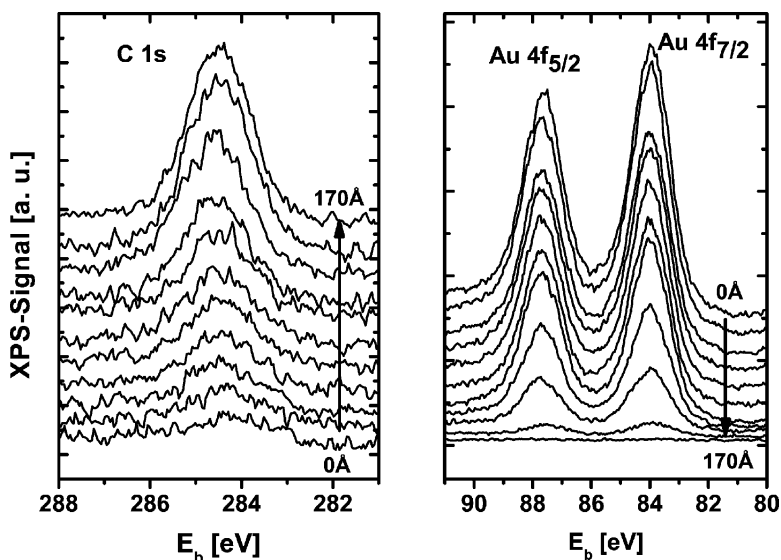


Fig. 7. XPS spectra C 1s and Au 4f as a function of evaporated P4P on the carbon-covered gold surface at 93 K. The mean thickness of P4P for the individual spectra can be deduced from Fig. 8.

A quite different behavior is obtained when the same experiment is carried out on a sample at room temperature (Fig. 9). After a relatively fast initial decrease at low coverage, caused by the formation of the monolayer (wetting layer), the Au 4f signal levels off and decreases rather slowly after that point. Even at a mean thickness of 67 nm, about 40% of the Au 4f signal is still

retained. This suggests that the subsequent multilayers grow in form of high islands, exposing large areas of the gold surface (only covered by the monolayer) even at a rather large mean thickness of P4P. Therefore, at room temperature the growth mode is clearly of the Stranski–Krastanov type. In Fig. 10, an optical micrograph shows the islands on the polycrystalline gold surface after

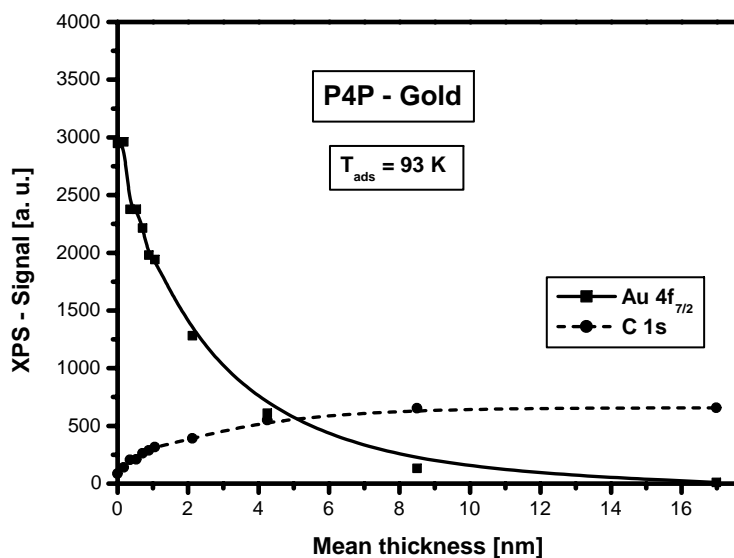


Fig. 8. Change of the C 1s and Au 4f<sub>7/2</sub> XPS signal during evaporation of P4P on the initially carbon-covered gold surface at 93 K.

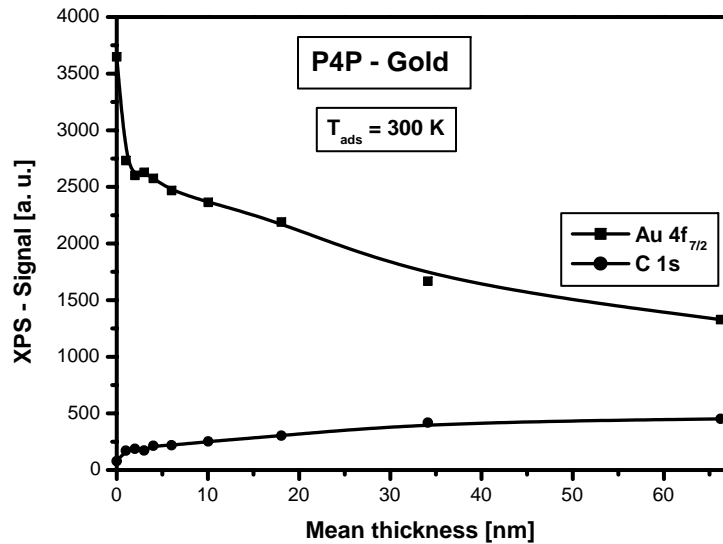


Fig. 9. Change of the C 1s and Au 4f<sub>7/2</sub> XPS signal during evaporation of P4P on the initially carbon-covered gold surface at 300 K.

evaporation of 30 nm P4P at room temperature. Highly oriented, needle-like islands are created on the individual crystallites of the polycrystalline gold substrate. The self-assembling of oligo-penylenes to form needle-like structures is an inherent property of these materials and has been frequently observed on various single-crystalline substrates [5,13,39].

### 3.3. Combined XPS and TDS experiments

In the previous part, we have described that the growth mode of the multilayer depends strongly on the substrate temperature. While at 93 K a continuous layer-like growth is observed (probably amorphous), at room temperature the thin film clearly grows in

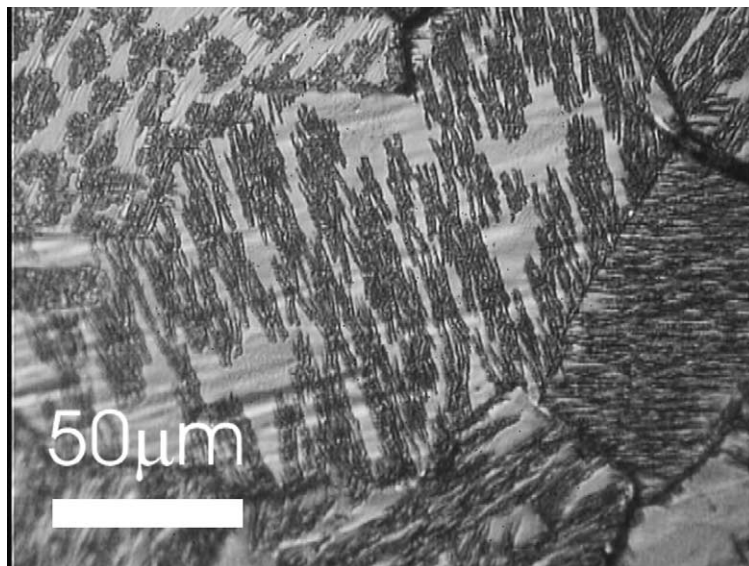


Fig. 10. Optical micrograph of the recrystallized gold surface covered with P4P of 30 nm mean thickness. Film grown at 300 K.

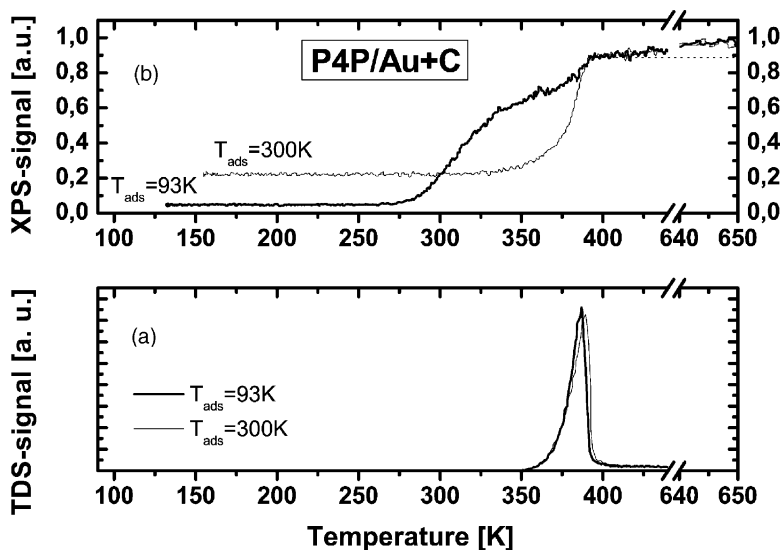


Fig. 11. Desorption of P4P after adsorption on the initially carbon-covered Au surface. Change of the QMS signal (a) and the Au  $4f_{7/2}$  XPS signal (b) during heating, for two different adsorption temperatures: 93 and 300 K. In the latter case the sample was cooled after layer preparation at 300 K and the experiment was started at low temperature. Initial mean layer thickness in both cases: 7 nm.

form of (crystalline) islands [13]. The shape and the peak maxima of the thermal desorption spectra, however, are only slightly influenced by the adsorption temperature at equivalent coverage. This suggests that—prior to desorption—a rearrangement of the layer commences, which leads to nearly equivalent structural conditions when desorption takes place, independent of the initial structure. In order to study this rearrangement in detail, we have performed simultaneous desorption and XPS measurements, both on the clean and on the carbon-covered gold surface. In Fig. 11a, desorption spectra are shown after adsorption of thin P4P films of about 7 nm mean thickness on a carbon-covered surface at room temperature and at 93 K, respectively. Within the achievable reproducibility of the film thickness, both spectra are nearly identical (although a small but reproducible difference in the peak maxima can be observed for room temperature and low temperature adsorption). In Fig. 11b, the Au  $4f_{7/2}$  XPS signals are plotted as a function of the surface temperature for the same P4P layers grown at different temperatures (heating rate 1 K/s). For the layer prepared at room temperature a significant gold signal can still be observed due to the island formation described above. In this particular case the sample was cooled down to 93 K after layer preparation at room temperature. Sample heating was started at low

temperature for both cases. No change in the Au 4f signal was found in the whole temperature range until at about 340 K desorption of P4P starts. This results in an increase of the XPS signal until all molecules in the multilayer are desorbed (at 400 K). Finally, the XPS Au 4f signal increases slightly during desorption of the monolayer until the signal of the clean gold surface is reached (at 650 K).

A different evolution of the gold XPS signal is observed if the same experiment is performed after layer formation at 93 K. Evaporation of the same amount (7 nm) of P4P leads to a nearly complete suppression of the gold signal. However, the gold signal starts to reappear during heating of the sample already at a temperature of about 270 K, although no significant desorption can be observed in this temperature range. Apparently, this is due to a recrystallisation of the P4P multilayer, from an originally continuous to an island shaped film. Above a temperature of about 330 K the increase of the XPS signal levels off, although in this temperature range desorption already starts. Only at the very end of the multilayer desorption (at about 390 K), the XPS signal once more increases rapidly and reaches the value characteristic of the gold surface, covered with the remaining monolayer. A slight further increase of the Au 4f signal finally appears during desorption of the monolayer at higher temperature.

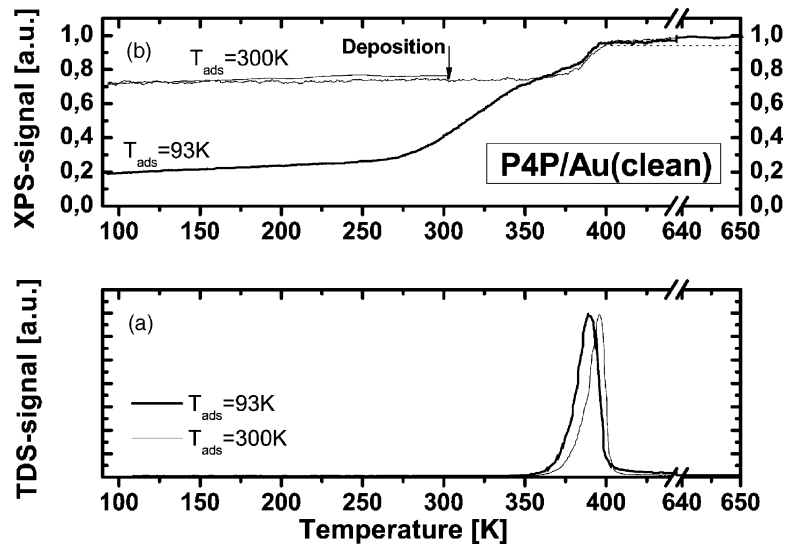


Fig. 12. Desorption of P4P after adsorption on the initially clean gold surface. Change of the QMS signal (a) and the Au  $4f_{7/2}$  XPS signal (b) during heating, for two different adsorption temperatures: 93 and 300 K. Again, in the latter case the sample was cooled after adsorption at 300 K. Initial mean layer thickness in both cases: 7 nm.

There are two features in these data which need a more detailed discussion. First, why does the XPS signal not change very much when desorption already takes place (between 340 and 380 K)? At this stage the layer consists of rather high islands which cover just about 25% of the total surface area (estimated from the Au 4f signals before and after desorption). As the mean layer thickness is 7 nm, the average height of the islands can be estimated to be about 28 nm. Desorption apparently proceeds mainly from the tops of the islands leaving the covered substrate surface more or less unchanged. Since the mean free path of the Au 4f electrons is about 2.4 nm, as mentioned above, the detected Au 4f signal increases significantly only when the last 10% of P4P in the island shaped multilayer desorb. The second surprising feature of the evolution of the Au 4f signal during heating of the layer produced at 93 K is the increase of the signal *even beyond that* for the layer produced at 300 K, occurring above room temperature. Apparently, upon heating of the continuous film the layer rearranges to islands, which are considerably higher than those directly obtained at 300 K adsorption temperature. This suggests that the film grown at 300 K is metastable, with islands of lower height and therefore with larger surface areas covered by P4P. We have shown, that an adsorption temperature

of 330 K is needed in this case to get the thermodynamically stable island formation, which amounts to about 75% of the surface free from P4P islands.

The same experiment performed on the initially clean gold surface yields some significant differences in the layer growth (Fig. 12). For both adsorption temperatures (93, and 300 K), the XPS signal after P4P adsorption is larger compared to the previously discussed case. In particular, for adsorption at 300 K the XPS signal indicates already the formation of the thermodynamically stable islands. This indicates that the mobility of the P4P molecules is much higher on the initially clean gold surface. Even at a surface temperature of 93 K some island formation takes place already during P4P deposition, as can be deduced from the observation that for the 7 nm thick layer still about 20% of the original Au 4f signal can be detected.

#### 4. Summary

Adsorption of *p*-quaterphenyl on a polycrystalline gold surface proceeds in form of a monolayer (wetting layer) and a multilayer. The monolayer is strongly influenced by the surface cleanliness. On the clean gold surface, partial dissociation of P4P takes place

during sample heating. Up to 0.07 nm mean thickness all P4P dissociates, leading to desorption of hydrogen at 800 K and carbon in graphitic form remaining on the surface. For P4P in the coverage range between 0.07 and 0.15 nm, a branching into intact desorption of P4P and dissociation can be seen. The latter leads to hydrogen desorption around 650 K and graphitic carbon on the surface. Adsorbed P4P between 0.15 and 0.27 nm desorbs intact from the surface. On the carbon-covered gold surface no dissociation of P4P takes place. The monolayer mean thickness is about 0.27 nm, for both the clean and carbon-covered surface, indicating the presence of flat lying molecules in the first layer. After saturation of the monolayer a multilayer is formed which desorbs around 360 K with zero-order reaction. The desorption energy for multilayer desorption is 1.64 eV.

The morphology of the multilayer depends on the adsorption temperature and on the carbon contamination. At and above room temperature island growth of P4P is observed, whereas at 93 K the multilayer grows in form of a continuous film. This continuous layer transforms into an island shaped layer during heating of the sample, long before desorption starts. This implies that care has to be taken when trying to investigate the morphology of organic thin films grown at low temperature, e.g. by AFM or STM at room temperature. The mobility and therefore the probability of island formation is larger on the initially clean gold surface than on the carbon-covered surface. These findings are important for the tailoring of the actual thin film morphology of quaterphenyl on gold surfaces.

## Acknowledgements

This work has been supported by the Austrian “Fonds zur Förderung der wissenschaftlichen Forschung”, Proj. No. P15625. The authors would like to thank R. Saf and G. Hayn for analyzing the chemical purity of the used material.

## References

- [1] S. Tasch, C. Brandstaetter, F. Meghdadi, G. Leising, G. Froyer, L. Athouel, *Adv. Mater.* 9 (1997) 33.
- [2] M. Era, T. Tsutsui, S. Saito, *Appl. Phys. Lett.* 67 (1995) 2436.
- [3] D.J. Gundlach, Y.Y. Lin, T.N. Jackson, D.G. Schlom, *Appl. Phys. Lett.* 71 (1997) 3853.
- [4] M. Mobus, N. Karl, T. Kobayashi, *J. Cryst. Growth* 116 (1992) 495.
- [5] A. Andreev, G. Matt, C.J. Brabec, H. Sitter, D. Badt, H. Seyringer, et al., *Adv. Mater.* 12 (2000) 629.
- [6] E. Zojer, N. Koch, P. Puschnig, F. Meghdadi, A. Niko, R. Resel, et al., *Phys. Rev. B* 61 (2000) 16538.
- [7] L. Athouel, G. Froyer, M.T. Riou, M. Schott, *Thin Solid Films* 274 (1996) 35.
- [8] H. Yanagi, S. Okamoto, T. Mikami, *Synth. Met.* 91 (1997) 91.
- [9] N. Koch, L.M. Yu, V. Parente, R. Lazzaroni, R.L. Johnson, G. Leising, et al., *Adv. Mater.* 10 (1998) 1038.
- [10] R. Resel, G. Leising, *Surf. Sci.* 409 (1998) 302.
- [11] R. Resel, N. Koch, F. Meghdadi, G. Leising, W. Unzog, K. Reichmann, *Thin Solid Films* 305 (1997) 232.
- [12] Y. Yoshida, H. Takiguchi, T. Hanada, N. Tanigaki, E.M. Han, K. Yase, *Appl. Surf. Sci.* 130/132 (1998) 651.
- [13] F. Balzer, H.G. Rubahn, *Surf. Sci.* 507–510 (2002) 588.
- [14] B. Mueller, T. Kuhlmann, K. Lischka, H. Schwer, R. Resel, G. Leising, *Surf. Sci.* 418 (1998) 256.
- [15] C.B. France, B.A. Parkinson, *Appl. Phys. Lett.* 82 (2003) 1194.
- [16] M.G. Ramsey, D. Steinmueller, M. Schatzmayr, M. Kiskinova, F.P. Netzer, *Chem. Phys.* 177 (1993) 349.
- [17] E. Ito, H. Oji, M. Furuta, H. Ishii, K. Oichi, Y. Ouchi, et al., *Synth. Met.* 101 (1999) 654.
- [18] P. Puschnig, C. Ambrosch-Draxl, *Phys. Rev. B* 60 (1999) 7891.
- [19] E. Umbach, K. Gloeckler, M. Sokolowski, *Surf. Sci.* 402–404 (1998) 20.
- [20] F.S. Tautz, S. Sloboshanin, V. Shklover, R. Scholz, M. Sokolowski, J.A. Schaefer, et al., *Appl. Surf. Sci.* 166 (2000) 363.
- [21] U. Stahl, D. Gador, A. Soukopp, R. Fink, E. Umbach, *Surf. Sci.* 414 (1998) 423.
- [22] J. Taborski, V. Wuestenhagen, P. Vaeterlein, E. Umbach, *Chem. Phys. Lett.* 239 (1995) 380.
- [23] E. Umbach, M. Sokolowski, R. Fink, *Appl. Phys. A* 63 (1996) 565.
- [24] S. Lukas, S. Vollmer, G. Witte, C. Woell, *J. Chem. Phys.* 114 (2001) 10123.
- [25] S. Prato, L. Floreano, D. Cvetko, V. De Renzi, A. Morgante, S. Modesti, et al., *J. Phys. Chem. B* 103 (1999) 7788.
- [26] Y. Delugeard, J. Desuiche, J.L. Baudour, *Acta Cryst. B* 32 (1976) 702.
- [27] K. Irakura, <http://webbook.nist.gov/chemistry/3d-structs>.
- [28] J.L. Baudour, Y. Delugeard, P. Rivet, *Acta Cryst. B* 34 (1978) 625.
- [29] S. Müllegger, I. Salzmann, R. Resel, G. Hlawacek, C. Teichert, A. Winkler, *Phys. Rev. B*, submitted for publication.
- [30] D.A. King, *Surf. Sci.* 47 (1975) 384.
- [31] D.H. Parker, M.E. Jones, B.E. Koel, *Surf. Sci.* 233 (1990) 65.
- [32] P.A. Redhead, *Vacuum* 12 (1962) 203.

- [33] K.R. Paserba, A.J. Gellman, *Phys. Rev. Lett.* 86 (2001) 4338.
- [34] S.Yu. Krylov, L.J.F. Hermans, *Phys. Rev. B* 65 (2002) 092205–092251.
- [35] A.A. Balepin, V.P. Lebedev, E.A. Mirosnichenko, G.L. Koldobskii, V.A. Ostovskii, B.P. Larionov, B.V. Gidasov, Y.A. Lebedev, Energy effects in polyphenylenes and phenyl-tetrazoles, *Svoistva Veshchestv Str. Mol.* (1977) 93–98.
- [36] C.D. Wagner, W.M. Riggs, L.E. Davis, J.F. Moulder, G.E. Muilenberg, *Handbook of X-ray photoelectron spectroscopy*, Perkin Elmer Corp., 1978.
- [37] P.G. Schroeder, M.W. Nelson, B.A. Parkinson, R. Schlaf, *Surf. Sci.* 459 (2000) 349.
- [38] S. Li, E.T. Kang, K.G. Neoh, Z.H. Ma, K.L. Tan, W. Huang, *Appl. Surf. Sci.* 181 (2001) 201.
- [39] T. Mikami, H. Yanagi, *Appl. Phys. Lett.* 73 (1998) 563.